Communication

Mutual Coupling Compensation in Receive-Mode Antenna Array Based on Characteristic Mode Analysis

Dong-Woo Kim and Sangwook Nam

***Abstract*— In this communication, the characteristic mode analysis (CMA) is applied to the analysis of mutual coupling in a receive-mode antenna array with geometric symmetry. Because CMA provides modes that incorporate a mutual coupling effect, CMA can be used to develop a method for compensating this mutual coupling effect. An understanding of the symmetries and underlying physical characteristics of the characteristic modes (CMs) of a receive-mode antenna can be used to intuitively explain the effects of incident signal polarization and incidence angle on the port signal. Using this knowledge, a mutual coupling compensation matrix (MCCM) is constructed by finding the CMs and Z-matrix of a metallic antenna array through a single simulation. The proposed method is validated by comparing MCCM-predicted with simulated port currents on a 1-D linear bowtie antenna array model. Further validation revealed that the proposed MCCM significantly reduced the compensation error and outperformed the commonly used open-circuit voltage-based MCCM in providing accurate direction-of-arrival estimation results.**

***Index Terms*— Characteristic mode analysis (CMA), mutual coupling compensation, receive-mode antenna array.**

I. Introduction

Adaptive antenna array performance is affected by the distortion of incoming signal information through the mutual coupling between element antennas [1], which is induced by scattering between adjacent antennas in the receiving mode. Many attempts have been made to address the mutual coupling problem, which involves the development of methods to convert coupled measurable port signals into uncoupled port signals by constructing a mutual coupling compensation matrix (MCCM). Several electromagnetic compensation methods for constructing the MCCM have been proposed [1]–[4]. One of the best known of these methods is the open-circuit voltage (OCV) method [1], in which the MCCM is calculated from the equivalent network system of an antenna array. However, this method is somewhat inaccurate because its assumption of decoupled OCVs is inconsistent with actual situations. To overcome this problem, some researchers have suggested MCCMs based on other approaches, including method of moments (MoM) matrices [2], received mutual impedances [3], and induced electromotive force [4]. Although these approaches outperform the OCV method, they still have several disadvantages, including the need for multiple simulations, limitation in the antenna shapes that can be modeled, and, in particular, a lack of the physical perspective needed to analyze phenomena pertaining to multiple cases.

The characteristic mode analysis (CMA) can be a useful approach to overcoming these problems. CMA has been used in several applications, including the analysis of the scattering problem [5], mobile antenna design [6], and platform-mounted multi-in multi-out antenna design [7]. It has also been applied to finite-antenna arrays [8]–[10]. In [8], a characteristic port mode theory defined in terms of an N-port network [11] was used to calculate array excitation taper. In [9], a method for obtaining CMA on an isolated-element antenna from the entire antenna array structure including the mutual coupling effects was proposed. In [10], CMA was conducted for a 2×2 finite-antenna array.

While the CMA approaches in [8]–[10] involve port-shorting analysis of transmit-mode antenna arrays, to date, there has been no clear method developed for applying CMA to receive-mode antenna arrays in order to analyze the mutual coupling effects in the receiving mode. The main objective of this communication is to discuss how to incorporate CMA into mutual coupling compensation methodology to overcome the disadvantages of existing compensation methods. To do so, a model for applying CMA to the analysis of receive-mode antenna arrays based on an equivalent N-port antenna array network system is suggested. A CMA-based MCCM is then constructed based on two assumptions that: a finite number of characteristic modes (CMs) contribute to the mutual coupling and the incoming signal arrives from the specific elevation angle. As the proposed MCCM incurs endurable errors in cases in which there is a deviation from these assumptions, the underlying physical basis of the CMA is used to analyze the source of these errors.

The rest of this communication is organized as follows. In Section II, the background theory is reviewed. In Section III, a receive-mode antenna array is analyzed using CMA. In Section IV, the proposed MCCM is derived and evaluated, and finally, conclusions regarding the findings are given in Section V.

II. Background Theory

A. Equivalent Network System of Receive-Mode Antenna Array

Because the coupling paths of transmitting and receiving arrays differ, there have been some questions as to whether conventional array transmit-mode network parameters (Z-, Y-, and S-parameters) should be used in the analysis of mutual coupling in the receiving mode [12]. However, recent research has shown that the conventional network parameters for the transmitting mode can be successfully used for the exact analysis of receive-mode antenna array response [13]. An arbitrary N-element antenna array can be modeled as an N-port equivalent network $[\mathbf{Z}_\mathrm{A}] \in \mathbb{C}^{\mathrm{N}\times\mathrm{N}}$ with a load network $[\mathbf{Z}_\mathrm{L}] \in \mathbb{C}^{\mathrm{N}\times\mathrm{N}}$, in which an incoming signal generates OCVs at the ports of the antenna array $\mathbf{V}_\mathrm{oc} \in \mathbb{C}^{\mathrm{N}\times 1}$. The resulting receiving array system is equivalent to the network model shown in Fig. 1. From this equivalent network system, the relationship between the OCVs

Manuscript received February 20, 2018; revised June 18, 2018; accepted August 26, 2018. Date of publication September 10, 2018; date of current version November 30, 2018. This work was supported by Institute for Information & communications Technology Promotion (IITP) grant funded by the Korea government (MSIT) (No.2016-0-00130,Cloud based SW platform development for RF design and EM analysis). *(Corresponding author: Sangwook Nam.)*

The authors are with the Department of Electrical and Computer Engineering, Institute of New Media and Communication, Seoul National University, Seoul 152-742, South Korea (e-mail: cb3403@snu.ac.kr; snam@snu.ac.kr).

Color versions of one or more of the figures in this communication are available online at http://ieeexplore.ieee.org.

Digital Object Identifier 10.1109/TAP.2018.2869431

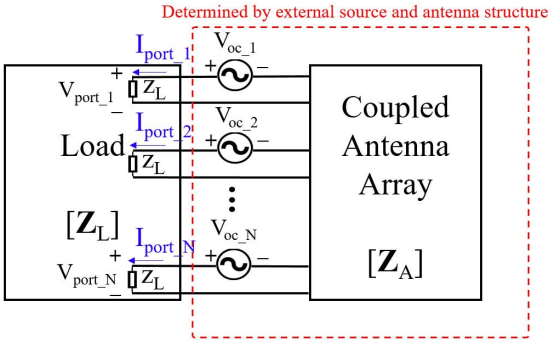

Fig. 1. Equivalent network system of a receive-mode N-element antenna array.

$\mathbf{V}_{\rm oc}$ and the port currents $\mathbf{I}_{\rm port} = [I_{\rm port\_1} I_{\rm port\_2} \ldots I_{\rm port\_N}]^{\rm T} \in \mathbb{C}^{\rm N\times 1}$ is obtained as

$$\mathbf{I}_{\rm port} = -[\mathbf{Z}_{\rm A} + \mathbf{Z}_{\rm L}]^{-1}\mathbf{V}_{\rm oc}. \tag{1}$$

Equivalently, the relationship between the coupled measurable port currents and the short-circuit currents $\mathbf{I}_{\rm sc} = [I_{\rm sc_1} I_{\rm sc_2} \ldots I_{\rm sc\_N}]^{\rm T} \in \mathbb{C}^{\rm N\times 1}$ is obtained as follows:

$$\mathbf{I}_{\rm port} = [\mathbf{Z}_A + \mathbf{Z}_{\rm L}]^{-1}\,[\mathbf{Z}_{\rm A}]\mathbf{I}_{\rm short}. \tag{2}$$

Similar to the OCVs $\mathbf{V}_{\rm oc}$, the short-circuit currents $\mathbf{I}_{\rm short}$ can be interpreted as sources generated by an incoming signal when all of the antenna ports are shorted. However, as the short-circuit currents are distorted by the mutual coupling between adjacent short-circuit antenna elements, it is necessary to use tools such as CMA to further analyze the short-circuit currents.

B. Characteristic Mode Analysis

CMA involves the eigenvalue analysis of the MoM Z-matrix of a conductor to produce the nth characteristic currents $\mathbf{J}_{\rm n} \in \mathbb{R}^{\rm M\times 1}$ and their respective eigenvalues $\lambda_{\rm n} \in \mathbb{R}$, where M($\gg N$) is the number of MoM basis functions. Using the CMA results, the current flowing on an arbitrary conductor $\mathbf{J} \in \mathbb{C}^{\rm M\times 1}$ can be decomposed into the characteristic currents $\mathbf{J} = \sum_{\rm n} (V_n^i/(1 + j\lambda_{\rm n}))\mathbf{J}_{\rm n}$, where the weighting of each current is called the modal weighting coefficient, $V_n^i = \mathbf{J}_{\rm n}^{\rm T}\mathbf{E}^{\rm inc} \in \mathbb{C}$ is the modal excitation coefficient (MEC), and $|1/(1 + j\lambda_{\rm n})|$ is called the modal significance. The characteristic currents in a symmetric structure can be decomposed into even and odd CMs, which are, respectively, defined as the CMs generated by sources with even and odd functional distributions relative to an axis perpendicular to the plane of symmetry [7], [14]. This axis of symmetry serves as the perfect magnetic conductor and perfect electric conductor walls for the even and odd CMs, respectively, which is used in the coupled line theory [15]. It should be noted that this definition of even and odd CMs is different from the definition based on the shape of the current distribution used in [16].

In the case of a transmit-mode antenna, CMA is carried out by modeling a structure with the antenna ports shorted. By contrast, a receive-mode antenna must be modeled under the fact that there is a load on the port, which makes the application of CMA difficult because the CMs will no longer be orthogonal in this case [17]. Here, we address this problem by modeling a receive-mode antenna array as Norton's equivalent N-port network, which enables to use the CMA to obtain the short-circuit currents generated by an incoming signal for the entire structure of a short-circuit ($Z_{\rm L} = 0\ \Omega$) antenna array. This, in turn, allows the received port signals to be analyzed by calculating the results of (2) with the short-circuit current represented as the CMs.

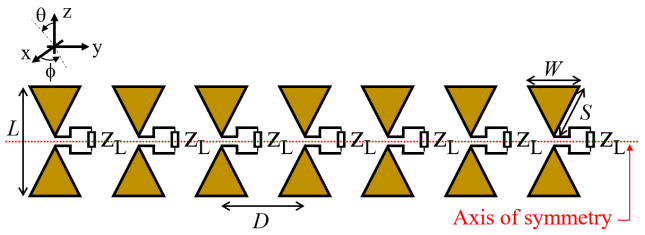

Fig. 2. Geometry of a bowtie receiving array with seven antenna elements. W = 19.22 mm ($=\lambda_0/6.5$), S = 20.93 mm ($=\lambda_0/6$), and L = 38.44 mm ($=\lambda_0/3.25$), where λ_0 is the wavelength at 2.4 GHz.

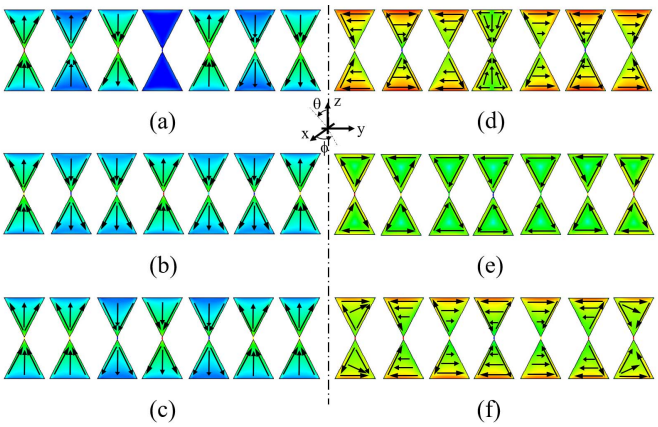

Fig. 3. Simulated current distribution of short-circuit bowtie antenna array at 2.4 GHz. (a) Mode 1. (b) Mode 2. (c) Mode 3. (d) Mode 13. (e) Mode 14. (f) Mode 15.

As discussed earlier, receive-mode antenna array CMA covers the entire short-circuit antenna structure, resulting in CMs that reflect the coupling effect between all element antennas. Accordingly, the information produced by the CMA can be used to analyze or compensate the mutual coupling effects in the array. This physical basis for the CMA results can be used to further investigate how to compensate the mutual coupling, as will be explained further in Section III.

III. CMA of Receive-Mode Bowtie Antenna Array

A. Bowtie Antenna Array Configuration

The configuration of a bowtie antenna array is shown in Fig. 2. The uniformly linear array comprises seven identical elements of the antenna. The bowtie element is designed to operate in the 2.4 GHz industrial scientific medical band and to be matched at 50 Ω termination in an isolated environment. In this section, the antenna spacing D is fixed to the electrical length $\lambda_0/2$ at 2.4 GHz, giving the adjacent elements a high coupling of about −14 dB. The simulation and analysis were carried out at the single frequency of 2.4 GHz using the FEKO 2017 [18].

B. CMA of the Short-Circuit Bowtie Antenna Array

Although as many CMs as possible should be used to represent the exact current distribution induced by an incoming signal, in practice, the CM's limited eigenvalue dynamic range [19] means that only reliable CMs can be used. The FEKO simulator results shown in Fig. 3 provide 15 accurate CMs for the geometry of the bowtie antenna array. The eigenvalues for 15 CMs are −0.1, 0.12, −0.27, −0.40, 0.43, −0.48, 1.17, −24.3, −25.1, −26.8, −29.8, −35.6, −48.7, 95.6, and −100.5, respectively. As the structure of the array is bilaterally symmetric, the obtained CMs can be classified into odd

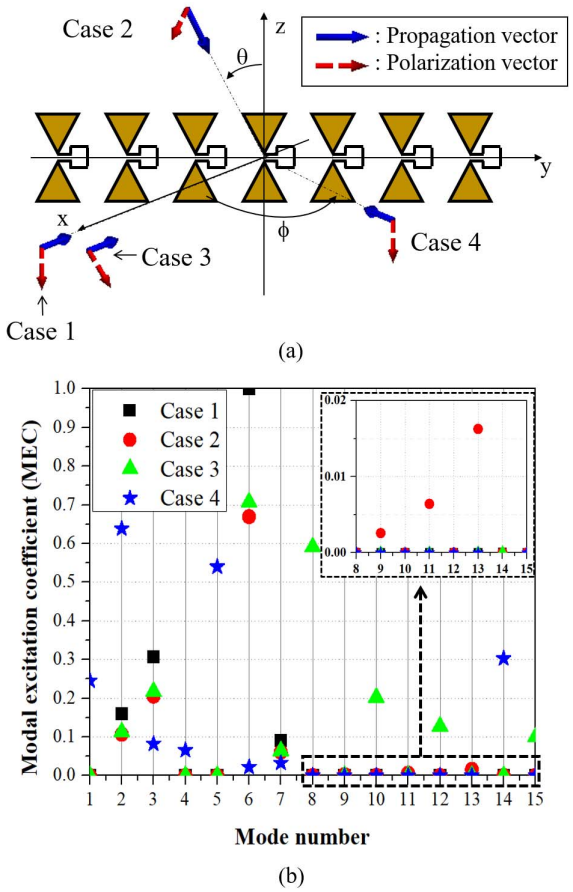

Fig. 4. Modal analysis of short-circuit bowtie antenna array for four incoming signal cases. (a) Configuration and (b) simulation results of MEC at 2.4 GHz.

(modes 1, 2, 3, 4, 5, 6, 7, and 14) and even (modes 8, 9, 10, 11, 12, 13, and 15) CMs. The current distribution on the conductor can be expressed as the sum of the characteristic currents, allowing the short-circuit currents $\mathbf{I}_{\text{short}}$ to also be expressed. However, the symmetry properties dictate that the odd CMs contribute to the generation of short-circuit currents while the even CMs do not. In addition, it is reasonable to ignore the higher order CMs above mode 15 because these are usually even modes, such as 13, 14, and 15, with inductive loop current distribution and therefore do not contribute to port signals.

C. Modal Analysis of Induced Short-Circuit Current by Incoming Signal

Fig. 4(a) illustrates a case in which an incoming plane-wave signal impinges on a short-circuit bowtie antenna array, generating a current on the antenna array with induced CM weights dependent on the direction and polarization of the incoming signal. To determine the relationship between the incoming signal and the induced CMs, four distinct cases are compared. Case 1 ($\phi = 0°$, $\theta = 90°$, and z-polarization) represents a reference incoming signal from the broadside direction; case 2 ($\phi = 0°$, $\theta = 30°$, and z-polarization) varies the elevation angle θ; case 3 ($\phi = 0°$, $\theta = 90°$, and 45°-tilted z-polarization) tilts the polarization; and case 4 ($\phi = 45°$, $\theta = 90°$, and z-polarization) varies the azimuth angle ϕ. The MECs of the antenna array's CMs are plotted in Fig. 4(b), from which it is seen that the incoming signals for cases 1 and 4 generate only odd CMs as a result of the symmetry properties, while cases 2 and 3 generate both odd and even CMs. These results suggest that tilting the elevation or polarization angle results in the increased production of even CMs. Furthermore, the most significant factor determining the weight of odd CMs is seen to be the azimuth angle of the incoming signal. (Although the elevation and polarization angles also change the weight of the odd CMs slightly, the effect is seen to be negligible.) Because the weight of the odd CMs determines the short-circuit current, it is inferred that the induced short-circuit current is determined by the azimuth angle of the incident signal.

IV. CMA-Based Mutual Coupling Compensation Matrix

A. Derivation of MCCM Based on CMA

Once the short-circuit antenna's CMA information has been extracted, the uncoupled port signal can be obtained. As mentioned previously, CMA can be used to approximate the current distribution on a short-circuit antenna $\mathbf{J}_{\text{short}} \in \mathbb{C}^{\text{M}\times 1}$ with P CMs as follows:

$$\mathbf{J}_{\text{short}} \simeq \sum_{\text{n}=1}^{\text{P}} \frac{\mathbf{J}_{\text{n}}^{T}\mathbf{E}^{\text{inc}}}{1+j\lambda_{\text{n}}}\mathbf{J}_{\text{n}} = [\mathbf{J}_{\text{CM}}][\Lambda]^{-1}[\mathbf{J}_{\text{CM}}]^{T}\mathbf{E}^{\text{inc}}. \tag{3}$$

where $[\mathbf{J}_{\text{CM}}] = [\mathbf{J}_1\ \mathbf{J}_2 \ldots \mathbf{J}_{\text{P}}] \in \mathbb{R}^{\text{M}\times\text{P}}$ is the set of characteristic current vectors, $[\Lambda] = \text{diag}(1+j\lambda_1, \ldots, 1+j\lambda_{\text{P}}) \in \mathbb{C}^{\text{P}\times\text{P}}$, and $\lambda_1 < \lambda_2 < \ldots < \lambda_{\text{P}}$. According to (2), only the short-circuit currents $\mathbf{I}_{\text{short}}$ contribute to the port currents $\mathbf{I}_{\text{port}}$. The required $\mathbf{I}_{\text{short}}$ can be extracted from (3) as follows:

$$\mathbf{I}_{\text{short}} \simeq \sum_{\text{n}=1}^{\text{P}} \frac{\mathbf{J}_{\text{n}}^{T}\mathbf{E}^{\text{inc}}}{1+j\lambda_{\text{n}}}\mathbf{I}_{\text{n}} = [\mathbf{I}_{\text{CM}}][\Lambda]^{-1}[\mathbf{J}_{\text{CM}}]^{T}\mathbf{E}^{\text{inc}} \tag{4}$$

where $\mathbf{I}_{\text{n}} = [I_{\text{n\_1}}\, I_{\text{n\_2}} \ldots I_{\text{n\_N}}]^{T} \in \mathbb{R}^{\text{N}\times 1}$ is the set of short-circuit currents of the nth CM at each port and $[\mathbf{I}_{\text{CM}}] = [\mathbf{I}_1\ \mathbf{I}_2 \ldots \mathbf{I}_{\text{P}}] \in \mathbb{R}^{\text{N}\times\text{P}}$ is the set of short-circuit current vectors for P CMs; among these, only the odd CMs contribute to the generation of short-circuit currents because as mentioned in Section III-B, $\mathbf{I}_{\text{n}}$ of an even CM is a zero vector. Thus, (4) can be reduced to

$$\mathbf{I}_{\text{short}} \simeq \sum_{m=1}^{O} \frac{\mathbf{J}_{m}^{odd\,T}\mathbf{E}^{\text{inc}}}{1+j\lambda_{m}^{odd}}\mathbf{I}_{m}^{odd} = [\mathbf{I}_{CM}^{odd}][\Lambda^{odd}]^{-1}[\mathbf{J}_{CM}^{odd}]^{T}\mathbf{E}^{\text{inc}} \tag{5}$$

where O is the number of odd CMs ($O < P$) and the columns of each matrix with the superscript "odd" are composed of O odd CM vectors, e.g., $[\mathbf{I}_{CM}^{odd}] = [\mathbf{I}_1^{odd} \ \cdots \ \mathbf{I}_{\text{O}}^{odd}] \in \mathbb{R}^{\text{N}\times\text{O}}$. In addition, using the properties of odd symmetry and assuming that a z-polarized signal impinges from the specific elevation angle ($\theta = 90°$), the inner product of the entire-domain vectors $\mathbf{J}_{\text{m}}^{\text{odd}\,T}\mathbf{E}^{\text{inc}}$ in (5) can be approximated as the inner product of two-port-domain vectors $c\mathbf{I}_{\text{m}}^{\text{odd}\,T}\mathbf{E}_{\text{port}}^{\text{inc}}$, where $\mathbf{E}_{\text{port}}^{\text{inc}}$ is the incident E-field across the port, which can be treated as an uncoupled port signal, and c is a complex constant. As shown in Fig. 5(c), this assumption leads to some error when the incoming signal is tilted along either the elevation or polarization angle. Nevertheless, using this assumption, (5) can be expressed as

$$\begin{aligned}\mathbf{I}_{\text{short}} &\simeq \sum_{m=1}^{O} \frac{c\mathbf{I}_{m}^{odd\,T}\mathbf{E}_{\text{port}}^{\text{inc}}}{1+j\lambda_{m}^{odd}}\mathbf{I}_{m}^{odd} \\ &= c[\mathbf{I}_{CM}^{odd}][\Lambda^{odd}]^{-1}[\mathbf{I}_{CM}^{odd}]^{T}\mathbf{E}_{\text{port}}^{\text{inc}}.\end{aligned} \tag{6}$$

The relationship between the measurable 50 Ω port currents and the uncoupled port signals can then be derived by substituting $\mathbf{I}_{\text{short}}$ from (6) into (2) and scaling $\mathbf{E}_{\text{port}}^{\text{inc}}$ by c, denoted by $\tilde{\mathbf{E}}_{\text{port}}^{\text{inc}}$, as

$$\mathbf{I}_{\text{port}} \simeq \underbrace{[\mathbf{Z}_{\text{A}} + \mathbf{Z}_{\text{L}}^{(50)}]^{-1}[\mathbf{Z}_{\text{A}}][\mathbf{I}_{CM}^{odd}][\Lambda^{odd}]^{-1}[\mathbf{I}_{CM}^{odd}]^{T}}_{[\mathbf{C}]}\tilde{\mathbf{E}}_{\text{port}}^{\text{inc}} \tag{7}$$

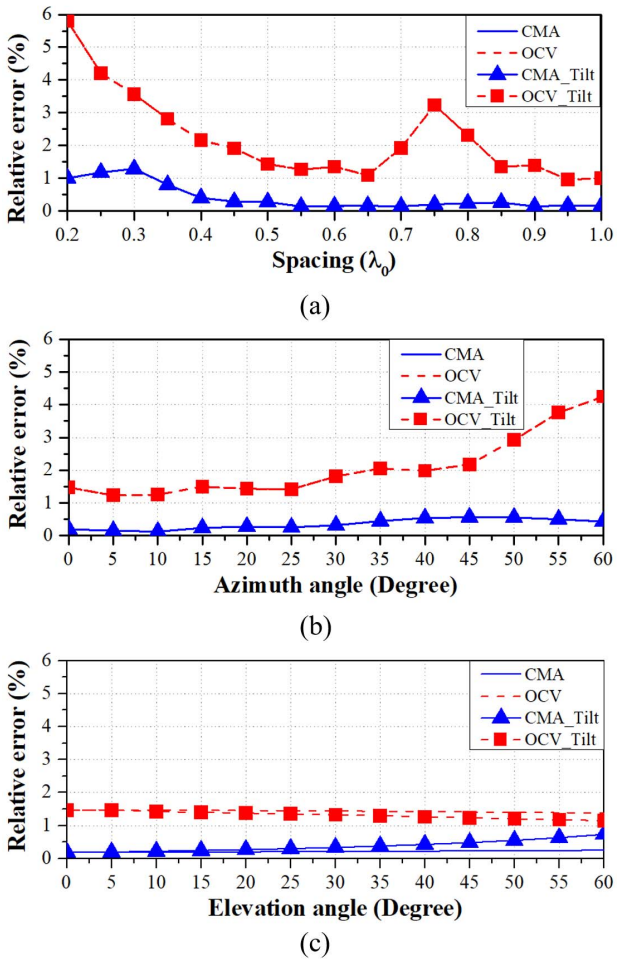

Fig. 5. Results of predicting coupled port currents at the 50 Ω port for given uncoupled port signals. (a) Relative error versus spacing. (b) Relative error versus azimuth angle. (c) Relative error versus elevation angle.

where $[\mathbf{C}] \in \mathbb{C}^{\mathrm{N}\times\mathrm{N}}$ is called the MCCM. Finally, the proposed MCCM [**C**] is obtained from the Z-matrix of the N-port antenna array and the data obtained from the CM simulation of the short-circuit antenna array. This can be done in a single run of a commercial CM simulator. From a physical standpoint, for a set of measured coupled port currents, the MCCM [**C**] matrix computes the uncoupled port currents by inversely calculating the weight of the odd CMs generated by the incoming signal.

B. Evaluation of the Proposed MCCM

The proposed MCCM was evaluated by comparing its predicted coupled port currents with those obtained from a 50 Ω loaded bowtie antenna array model. The uncoupled port signals produced by an incoming signal in a linear array can be treated as the normalized steering vector $\tilde{\mathbf{E}}^{\mathrm{inc}}_{\mathrm{port}}(\phi_i) = [1\ 1\cdot\exp\{j(2\pi d/\lambda)\sin(\phi_i)\}\ldots 1\cdot\exp\{j(N-1)(2\pi d/\lambda)\sin(\phi_i)\}]^{\mathrm{T}} \in \mathbb{C}^{\mathrm{N}\times 1}$. Using (7), the normalized predicted coupled port currents $\mathbf{I}^{\mathrm{P}}_{\mathrm{port}}$ were derived by multiplying and scaling MCCM [**C**]. For comparison, the actual normalized port currents $\mathbf{I}^{\mathrm{A}}_{\mathrm{port}}$ were obtained from a full-wave simulation in FEKO 2017. The degree of accuracy was determined from the following relative error:

$$\varepsilon_r = \frac{\|\mathbf{I}^P_{port} - \mathbf{I}^A_{port}\|_2}{\|\mathbf{I}^A_{port}\|_2} \times 100(\%). \tag{8}$$

Fig. 5 shows the results for three cases: 1) change in antenna spacing from 0.2 to 1λ_0; 2) change in azimuth angle ϕ from 0° to 60°; and 3) change in elevation angle θ from 0° to 60°. For each case, the results of the 45°-tilted z-polarization are also plotted. In cases 2) and 3), the antenna spacing D was fixed to the electrical length $\lambda_0/2$ at 2.4 GHz using the model described in Section III. For further comparison, the results produced by the well-known OCV-based MCCM are also shown. The OCV-based MCCM has errors greater than 1% in all three cases, primarily because it applies the OCV as the uncoupled port voltage, which is a very unrealistic assumption as the OCV already contains the effects of mutual coupling. By contrast, the proposed CMA-based MCCM yields accurate results with errors of below 1% in all three cases because it utilizes the relationship between the port and uncoupled signals. Nevertheless, it produces more errors in two cases. As shown in Fig. 5(a), the error increases when the element spacing is reduced because reducing the spacing between elements results in more dominant CMs, which makes it impossible to accurately express short-circuit currents with only 15 CMs. This is, however, unproblematic because antenna arrays are rarely designed with the spacing of less than 0.5λ_0. Fig. 5(c) shows a slight increase in error at somewhat increased tilting of the polarization and elevation angles. This occurs because the proposed MCCM assumes that the z-polarized signal is coming from specific elevation angle ($\theta = 90°$) and, as mentioned in Section III-C, results in a slight difference in the weight of the odd CMs. Once again, this error is insignificant in terms of compensation result reliability, as is verified in the following example of the direction-of-arrival (DOA) estimation.

C. Application Direction-of-Arrival Estimation

One of the more prominent examples of the application of mutual coupling compensation is DOA estimation. A number of algorithms are used to estimate DOA, including MUSIC [20], all of which apply a receiving signal model without mutual coupling

$$\mathbf{I}_{\mathrm{port}}(t) = [\mathbf{A}]\,\mathbf{s}(t) + \mathbf{n}(t) \tag{9}$$

where $\mathbf{s}(t) = [s_1(t)s_2(t)\ldots s_{\mathrm{K}}(t)]^T \in \mathbb{C}^{\mathrm{K}\times 1}$ is the incoming signal vector arriving at the antenna array from the distinct direction $(\theta_1, \phi_1), (\theta_2, \phi_2), \ldots, (\theta_K, \phi_K)$, $[\mathbf{A}] = [\boldsymbol{\alpha}(\phi_1)\ \boldsymbol{\alpha}(\phi_2)\ldots\boldsymbol{\alpha}(\phi_K)] \in \mathbb{C}^{\mathrm{N}\times\mathrm{K}}$ is a steering matrix comprising a steering vector with $\alpha(\phi_i) = [1\ \exp\{j(2\pi d/\lambda)\sin(\phi_i)\}\ldots\exp\{j(N-1)(2\pi d/\lambda)\sin(\phi_i)\}]^T \in \mathbb{C}^{\mathrm{N}\times 1}$, and $\mathbf{n}(t) = [n_1(t)n_2(t)\ldots n_{\mathrm{N}}(t)]^T \in \mathbb{C}^{\mathrm{N}\times 1}$ is the noise signal vector. A modified receiving signal model that reflects the mutual coupling effect was suggested in [21]

$$\mathbf{I}_{\mathrm{port}}(t) = [\mathbf{C}][\mathbf{A}]\mathbf{s}(t) + \mathbf{n}(t) \tag{10}$$

where $[\mathbf{C}] \in \mathbb{C}^{\mathrm{N}\times\mathrm{N}}$ is the MCCM. Based on (10), the generalized MUSIC algorithm including the mutual coupling effects was proposed in [21]

$$P_{\mathrm{MU}}(\phi) = \frac{1}{\left\|[\mathbf{E}^+_{\mathrm{N}}][\mathbf{C}]\boldsymbol{\alpha}(\phi)\right\|^2} \tag{11}$$

where $[\mathbf{E}^+_N]$ is the basis for the noise subspace and $P_{\mathrm{MU}}(\phi)$ is the spatial spectrum.

To obtain the accurate DOA estimation results using the generalized MUSIC algorithm, a rigorous MCCM [**C**] is required; accordingly, the DOA estimation ability of the proposed MCCM was validated by applying the modified MUSIC algorithm in (11) to three cases: one in which the proposed CMA-based MCCM was applied; one in which the conventional OCV-based MCCM was applied; and one in which mutual coupling effects were disregarded ([**C**] = [**I**]). The DOA estimation for the uniform linear bowtie antenna array with a spacing of $\lambda_0/2$ and a 50 Ω load shown in Fig. 2 was performed at 2.4 GHz with an SNR of 30 dB using 700 snapshots.

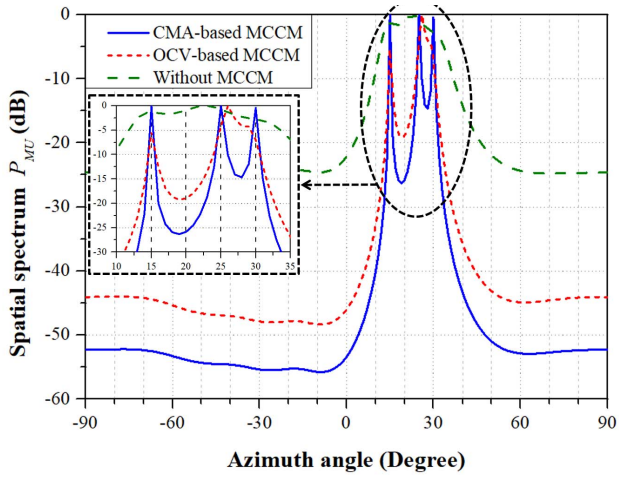

Fig. 6. MUSIC spectra for the estimation of three uncorrelated z-polarized incoming signals from $(\theta, \phi) = (90°, 15°)$, $(\theta, \phi) = (90°, 25°)$, and $(\theta, \phi) = (90°, 30°)$.

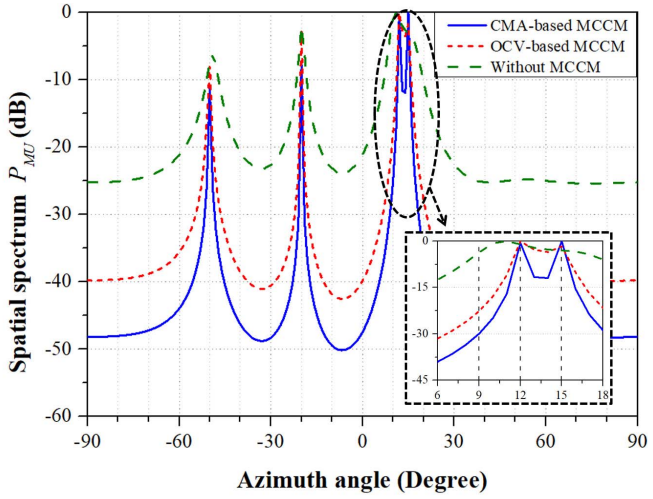

Fig. 7. MUSIC spectra for the estimation of four uncorrelated incoming signals from $(\theta, \phi) = (30°, -50°)$, $(\theta, \phi) = (30°, -20°)$, $(\theta, \phi) = (30°, 12°)$, and $(\theta, \phi) = (30°, 15°)$. All four incoming signals have elevation and polarization angles tilted by 60° and 45°, respectively.

Fig. 6 shows the DOA azimuth angle estimation results for three uncorrelated incoming signals with untilted elevation and polarization angles impinging from $(\theta, \phi) = (90°, 15°)$, $(\theta, \phi) = (90°, 25°)$, and $(\theta, \phi) = (90°, 30°)$. Fig. 7 shows the DOA estimation results when four uncorrelated incoming signals impinge from $(\theta, \phi) = (30°, -50°)$, $(\theta, \phi) = (30°, -20°)$, $(\theta, \phi) = (30°, 12°)$, and $(\theta, \phi) = (30°, 15°)$ with elevation and polarization angle tilts of 60° and 45°, respectively. The results in Figs. 6 and 7 confirm the accuracy of the CMA-based MCCM in terms of DOA estimation; in particular, Fig. 7 reveals the exact DOA estimation even though it represents close to the worst case, in which the error of the CMA-based MCCM is increased by the tilts in the elevation and polarization angles.

V. Conclusion

In this communication, a CMA-based mutual coupling compensation method for a receive-mode antenna array comprising symmetric antenna elements has been proposed and tested. The CMA-based MCCM has been derived by employing CMA in the modeling of a 1-D bowtie antenna array as an equivalent N-port network system. Although two assumptions have been made, the errors by these assumptions have been physically explained by CMA and are endurable in terms of compensation result reliability compared to the conventional OCV-based MCCM. Beyond bowtie arrays, the CMA-based MCCM can be applied to many metallic antennas arrays whose elements are open-ended and geometrically symmetric, including dipole and monopole arrays. Furthermore, it can be applied to not only uniformly spaced but also nonuniformly spaced antenna array.

References

[1] I. J. Gupta and A. A. Ksienski, "Effect of mutual coupling on the performance of adaptive arrays," *IEEE Trans. Antennas Propag.*, vol. AP-31, no. 5, pp. 785–791, Sep. 1983.

[2] C. K. E. Lau, R. S. Adve, and T. K. Sarkar, "Minimum norm mutual coupling compensation with applications in direction of arrival estimation," *IEEE Trans. Antennas Propag.*, vol. 52, no. 8, pp. 2034–2041, Aug. 2004.

[3] H. T. Hui, "Improved compensation for the mutual coupling effect in a dipole array for direction finding," *IEEE Trans. Antennas Propag.*, vol. 51, no. 9, pp. 2498–2503, Sep. 2003.

[4] S. Henault, Y. M. M. Antar, S. Rajan, R. Inkol, and S. Wang, "The multiple antenna induced EMF method for the precise calculation of the coupling matrix in a receiving antenna array," *Prog. Electromagn. Res. M*, vol. 8, pp. 103–118, 2009.

[5] R. F. Harrington and J. R. Mautz, "Theory of characteristic modes for conducting bodies," *IEEE Trans. Antennas Propag.*, vol. AP-19, no. 5, pp. 622–628, Sep. 1971.

[6] J. Won, S. Jeon, and S. Nam, "Identifying the appropriate position on the ground plane for MIMO antennas using characteristic mode analysis," *J. Eletromagn. Eng. Sci.*, vol. 16, no. 2, pp. 119–125, Apr. 2016.

[7] D.-W. Kim and S. Nam, "Systematic design of a multiport MIMO antenna with bilateral symmetry based on characteristic mode analysis," *IEEE Trans. Antennas Propag.*, vol. 66, no. 3, pp. 1076–1085, Mar. 2018.

[8] I. Tzanidis, K. Sertel, and J. L. Volakis, "Characteristic excitation taper for ultrawideband tightly coupled antenna arrays," *IEEE Trans. Antennas Propag.*, vol. 60, no. 4, pp. 1777–1784, Apr. 2012.

[9] D. J. Ludick and D. B. Davidson, "DGFM-enhanced theory of characteristic modes for finite antenna array analysis," in *Proc. Int. Workshop Comput. Electromagn. (CEM)*, Barcelona, Spain, Jun. 2017, pp. 5–6.

[10] A. A. Salih, Z. N. Chen, and K. Mouthaan, "Characteristic mode analysis and metasurface-based suppression of higher order modes of a 2×2 closely spaced phased array," *IEEE Trans. Antennas Propag.*, vol. 65, no. 3, pp. 1141–1150, Mar. 2017.

[11] J. Mautz and R. Harrington, "Modal analysis of loaded N-port scatterers," *IEEE Trans. Antennas Propag.*, vol. AP-21, no. 2, pp. 188–199, Mar. 1973.

[12] H.-S. Lui, H. T. Hui, and M. S. Leong, "A note on the mutual-coupling problems in transmitting and receiving antenna arrays," *IEEE Antennas Propag. Mag.*, vol. 51, no. 5, pp. 171–176, Oct. 2009.

[13] J. W. Wallace and R. Mehmood, "On the accuracy of equivalent circuit models for multi-antenna systems," *IEEE Trans. Antennas Propag.*, vol. 60, no. 2, pp. 540–547, Feb. 2012.

[14] B. Yang and J. J. Adams, "Systematic shape optimization of symmetric MIMO antennas using characteristic modes," *IEEE Trans. Antennas Propag.*, vol. 64, no. 7, pp. 2668–2678, Jul. 2016.

[15] D. M. Pozar, *Microwave Engineering*, 4th ed. Hoboken, NJ, USA: Wiley, 2005.

[16] M. Cabedeo-Fabres, "Systematic design of antennas using the theory of characteristic modes," Ph.D. dissertation, Univ. Politécn. Valencia, Valencia, Spain, 2007.

[17] R. F. Harrington, J. R. Mautz, and Y. Chang, "Characteristic modes for dielectric and magnetic bodies," *IEEE Trans. Antennas Propag.*, vol. AP-20, no. 2, pp. 194–198, Mar. 1972.

[18] Altair Engineering. *FEKO 2017*. Accessed: 2017. [Online]. Available: https://altairhyperworks.com/product/FEKO

[19] K. Schab, B. Yang, and J. Adams, "EFIE singularity treatments and their effects on characteristic mode dynamic range," in *Proc. 11th Eur. Conf. Antennas Propag. (EUCAP)*, Paris, France, Mar. 2017, pp. 2673–2675.

[20] R. O. Schmidt, "Multiple emitter location and signal parameter estimation," *IEEE Trans. Antennas Propag.*, vol. AP-34, no. 3, pp. 276–280, Mar. 1986.

[21] C.-C. Yeh, M.-L. Leou, and D. R. Ucci, "Bearing estimations with mutual coupling present," *IEEE Trans. Antennas Propag.*, vol. 37, no. 10, pp. 1332–1335, Oct. 1989.